

PHOTOVOLTAIC PERFORMANCE OF MEH-PPV:PCBM POLYMER SOLAR CELLS WITH AN INTEGRATION OF ZINC OXIDE (ZnO) NANOPARTICLES

Thet Thet Naing¹ Nyein Wint Lwin² Than Zaw Oo³

Abstract

The poly (2-methoxy-5-(2-ethyl hexyloxy)-1, 4-phenylenevinylene) (MEH-PPV) films were prepared by spin coating technique. Introducing additive (ZnO nanoparticles (ZnO-NPs) of size ~ 250 nm) and the optical properties of MEH-PPV polymer films were investigated by UV-vis spectrophotometry. Following the polymer film characterization, the organic solar cells using MEH-PPV based light absorber layer were fabricated and the effect of additive (ZnO-NPs) on the power conversion efficiency of the devices was investigated. The "dichlorobenzene" device outperformed the devices with other three rival solvents and its efficiency is as high as 0.112%. Despite having higher absorption in active layer with ZnO-NPs, the efficiency of this modified device underperformed the reference device (without ZnO-NPs) which is attributed to the restricted charge carrier transport and morphological perturbation. The additive concentrations have a strong impact on optical and surface morphological properties of the photoactive polymer films and thus on the photovoltaic performance of the devices.

Keywords: MEH-PPV:PCBM solar cells, additive (ZnO-NPs)

Introduction

The worlds' energy consumption is being generated through the combustion of fossil fuels. The world is under the threat of global warming because of using fossil fuels such as coal and oil. Today, the reflections of global warming on daily life are seen as climate change. The fossil fuel resources are limited and costly. The finite supply of traditional fossil fuels (oil, natural gas, coal, etc.) underscores the urgency of searching for alternative energy sources. The need to develop inexpensive renewable energy sources stimulates scientific research for efficient, low-cost photovoltaic devices. Types of renewable energy technologies are solar energy, geothermal energy, wind energy, bioenergy, ocean energy and hydropower. Solar energy is one of the most promising, available, renewable energy sources of all.

¹ Dr, Lecturer, Department of Physics, Monywa University

² Dr, Associate Professor, Department of Physics, University of Distance Education

³ Dr, Associate Professor, Department of Physics, University of Mandalay

Photovoltaic (PV) cells convert solar energy into electrical energy. Solar cells are usually divided into three main generations. The first generation solar cells are mainly based on silicon (Si) wafers. The silicon-based photovoltaics have outstanding advantages in both efficiency and lifetime with power conversion efficiencies (PCE) in excess of 25%. Second generation solar cells are thin-film solar cells which include amorphous silicon (a-Si), and cadmium telluride (CdTe), and copper indium gallium selenide (CIGS). Their typical performance is 10-15%. Third generation solar cells are organic heterojunction solar cells, dye sensitized solar cells (DSSC) and organic/inorganic hybrid solar cells. Organic solar cells have received attention due to their low-cost, easy processability, low weight, and mechanical flexibility. Their power conversion efficiencies have increased considerably from 0.001% in 1975 to 1% in 1986 and more recently to 8.13% in 2010.

The power conversion efficiencies of organic solar cells are lower than inorganic (Si) solar cells. Several attempts have been implemented in order to achieve the higher device efficiency. Tailoring and controlling the morphology of photoactive layer and charge transport within the interpenetrating networks plays a crucial role in increasing the device performance. The general approach to enhance charge carrier transport in organic polymer materials is to increase the mesoscopic order and crystallinity. A nanoscale interpenetrating network with crystalline order is the desirable architecture for photoactive layer of organic solar cells. In addition, the electronic bandgaps of the materials in the photoactive layer should be tuned to harvest more light from the solar spectrum.

In addition, incorporating inorganic nanoparticles into conjugated polymer matrices is an area of current interest in the fields of optoelectronics and photovoltaics. This approach can take advantages of the beneficial properties of both materials: superior optoelectronic properties of conjugated polymers and high electron mobility of inorganic semiconductors which would result in an improved device performance. Moreover, polymers are technologically advantageous owing to the ease of flexibility of processing devices in solution. There have been reports on polymer-inorganic hybrid solar cells using zinc oxide (ZnO) nanoparticles.

In a heterojunction between a polymer and a wide band gap semiconductor (e.g., MEH-PPV:PCBM/ZnO-NPs system), the electrons can diffuse from the polymer to the semiconductor. When the polymer is illuminated with photon of energy larger than band gap, electron-hole pairs are generated. The electrons are injected into the conduction band of the semiconductor and can move along the nanoparticles network. The nature of the charge transfer process depends on the optical properties of two materials as well as the surface properties of the nanoparticles. In short, selecting the appropriate solvent and introducing additives would be two strategies to modify the optical, electrical and morphological properties of the photoactive polymer layer, thereby modulating the photovoltaic performance of the polymer solar cells.

Experimental Details

This section details about (i) synthesis of ZnO-NPs and (ii) device fabrication and efficiency measurement.

Synthesis of ZnO-NPs

In the synthesis of ZnO nanoparticles, zinc acetate dihydrate $\text{Zn}(\text{CH}_3\text{COO})_2 \cdot 2\text{H}_2\text{O}$ (2.95 g) was first dissolved in methanol (125 ml) and another solution of potassium hydroxide (1.57 g) in methanol (65 ml) was prepared by dissolving potassium hydroxide. This solution was added dropwise to the zinc acetate solution at 60 °C under vigorous stirring. After 2 h and 15 min, nanoparticles started to precipitate and the solution became turbid. The heater and stirrer were removed after 2 h and 15 min. The ZnO nanoparticles settled at the bottom and the excess mother liquor was removed and the precipitate was washed twice with methanol (50ml). The ZnO nanoparticles powder was obtained. The experimental setup for synthesis of ZnO nanoparticle is shown in Fig. 1.

Device Fabrication and Efficiency Measurement

The fabrication steps for organic photovoltaic device are depicted in Fig. 2. The devices were fabricated on indium tin oxide (ITO) coated glass substrates which are used as the transparent electrodes. The indium tin oxide (ITO) glasses were cleaned by sequential ultrasonification in acetone, distilled

water and isopropyl alcohol (IPA) for 15 min consecutively and dried by nitrogen blow. Since ITO was coated throughout the glass substrate, etching had to be carried out to remove the ITO at the sides, leaving the only ITO in the center region as shown in Fig. 3(a). ITO surfaces were then treated by UV light in order to remove the organic contamination on the ITO surface. The ultrasonic cleaner and UV chamber used in our ITO cleaning processes are shown in Fig.3 (b) and (c) respectively. Fabricated OPV devices are shown in Fig. 3(d).

For the fabrication of MEH-PPV:PCBM solar cells with additive (ZnO-NPs) concentrations (4 wt%, 6 wt%, 8 wt% and 10 wt%), the bulk heterojunction blend solutions of MEH-PPV:PCBM (1:2 wt%) were prepared in dichlorobenzene. A thin layer of poly (3, 4- ethylenedioxythiophene):poly (styrenesulfonate) or (PEDOT:PSS) (Sigma Aldrich) was spin-coated at 3000 rpm for 60 s on pre-cleaned ITO glass plates.

Then the PEDOT:PSS coated substrate was annealed at 100 °C for 15 min. Subsequently, MEH-PPV:PCBM photoactive layer was spun-coat at 1000 rpm for 60 s on the top of PEDOT:PSS layer. The active layer thicknesses were in the range of 80 nm-100 nm as determined by a surface profiler (Tencor Alpha-Step IQ). After annealing at 130 °C for 8 min, the devices were completed by deposition of cathode aluminum (Al) (~ 100 nm) through a mask by thermal evaporation at a pressure of 10^{-6} Torr. The device active area was around 0.07 cm². Fig. 4(a) shows thermal evaporator (NTE 1000) for the deposition metal (Al) cathode.

The I-V curves of the devices were recorded under illumination of light intensity (100 mW/cm²). The photovoltaic efficiency of organic solar cells were evaluated from the J-V characteristics of the device. It was measured using a computer-controlled digital source meter (Keithley 2420) with a Newport solar simulator (A.M. 1.5, 100 mW/cm²). Light intensity was calibrated with a National Renewable Laboratory (NREL)-calibrated monocrystalline Silicon solar cell. Fig. 4(b) shows the experimental setup for the efficiency measurement of OPV devices.



Figure 1: Experimental setup for synthesis of ZnO nanoparticles.

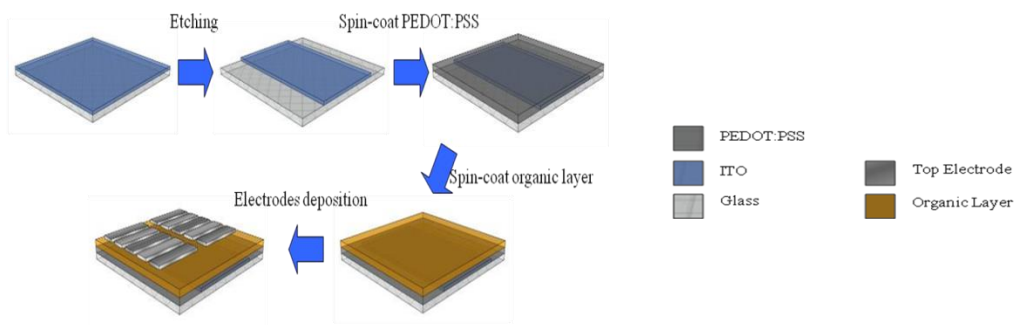


Figure 2: Fabrication steps for organic photovoltaic device.

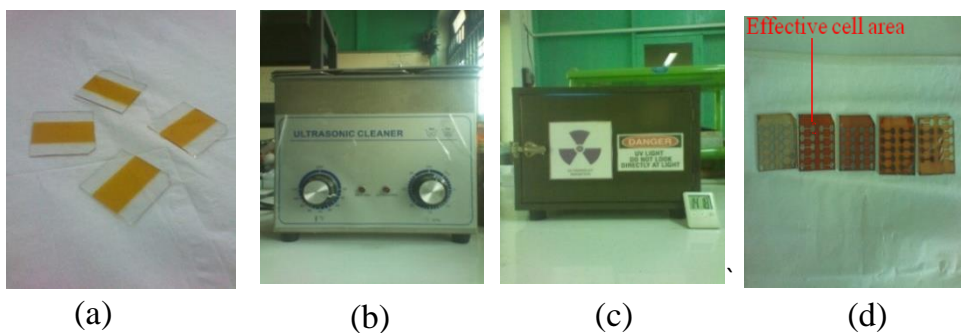
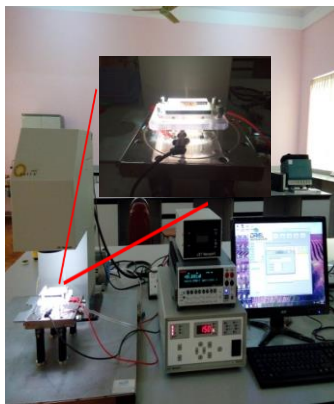


Figure 3: Illustrations of (a) etched ITO pattern on glass substrate, (b) ultrasonic cleaner, (c) UV chamber and (d) fabricated OPV devices.



(a)



(b)

Figure 4: (a) Thermal evaporator (NTE 1000) for the deposition metal (Al) cathode and (b) Experimental setup for the measurement of device efficiency (Newport Solar simulator and Keithley source meter).

Results and Discussion

This section discusses the effect of additive (ZnO-NPs) on photovoltaic performance of MEH-PPV:PCBM based organic solar cells.

Effect of Additive (ZnO-NPs) Concentration on Photovoltaic Performance of MEH-PPV/ZnO-NPs:PCBM Devices: Correlating the Properties and Performance

The device efficiencies of MEH-PPV:PCBM solar cells with additive (ZnO-NPs) concentrations (4 wt%, 6 wt%, 8 wt% and 10 wt%) were evaluated under A.M. 1.5 solar irradiation of intensity 100 mW/cm^2 . The J-V characteristics of MEH-PPV:PCBM/ZnO-NPs devices are shown in Fig. 5(a) and the measured device parameters are listed in Table 1. A reference MEH-PPV:PCBM solar cell produced a power conversion efficiency (η) of 0.112% with fill factor (FF) of 26.40, open circuit voltage (V_{oc}) of 0.63 V and short-circuit current density (J_{sc}) of 0.67 mA/cm^2 which outperformed the MEH-PPV:PCBM device with ZnO-NPs.

The V_{oc} of the reference devices is 0.63 V and those of the devices with ZnO-NPs are 0.58 V, 0.49 V, 0.63 V and 0.71 V for ZnO-NPs concentrations of 4 wt%, 6 wt%, 8 wt% and 10 wt% respectively. Higher V_{oc} of 0.71 V is produced in the device with ZnO-NPs (10 wt%) while lower V_{oc} of 0.49 V in the device with ZnO-NPs (6 wt%). The J_{sc} of the devices with ZnO-NPs is lower than that of reference device (67×10^{-2} mA/cm²) despite having higher absorption in MEH-PPV:PCBM active layer with ZnO-NPs. There may be some ZnO-NPs induced disturbances in electron path way towards the electron collecting electrode which reduces the J_{sc} . Among the devices with ZnO-NPs, the ZnO-NPs concentration of 8 wt% yields a higher J_{sc} which is consistent with the absorption data (Fig. 5(b)) that the absorption of active layer with ZnO-NPs (8 wt%) is higher than those with other ZnO-NPs concentrations (2 wt%, 4 wt% and 10 wt%). Step height profile of MEH-PPV:PCBM photoactive layer is shown in Fig. 6(a). The thickness of the film is about 230 nm. The roughness profiles of MEH-PPV:PCBM without and with ZnO-NPs are shown in Fig. 6(b).

FF is sensitive to the morphology and series resistance of the device. A gradual decrease of FF with increasing ZnO-NPs concentration is ascribed to an increased roughness of the film surface (Table 1). The series resistances (R_s) of the devices are calculated from the J-V curves of the devices and tabulated in Table 2. It is found that the R_s increase with increasing ZnO-NPs concentrations which would result in the lower FF of ZnO-NPs incorporated devices. To sum up, the efficiency lowering in the modified devices (with ZnO-NPs) despite having higher absorption with ZnO-NPs can be attributed to the restricted charge carrier transport and perturbed morphology.

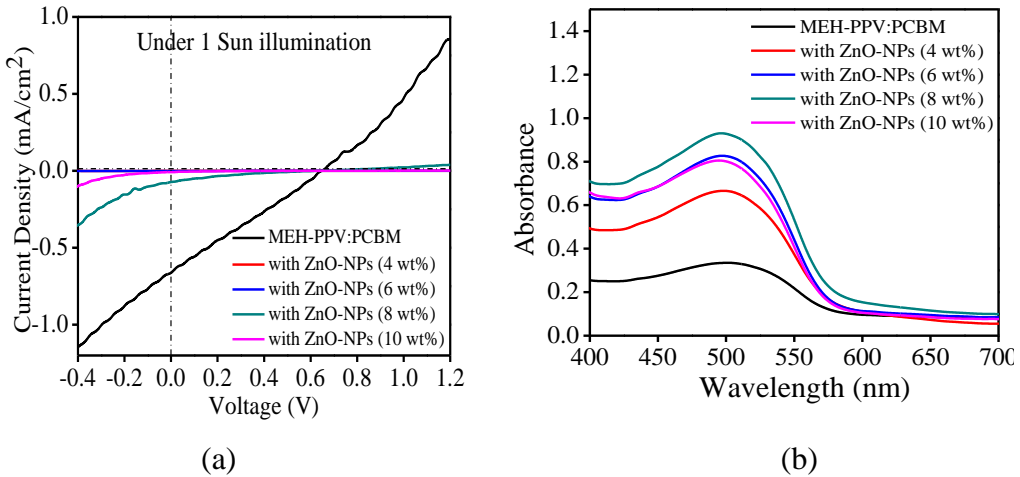


Figure 5: (a) J-V characteristics of the organic solar cells comprising MEH-PPV:PCBM/ZnO-NPs composite photoactive layer and (b) Absorption spectra of MEH-PPV:PCBM pure and MEH-PPV:PCBM/ZnO-NPs composite

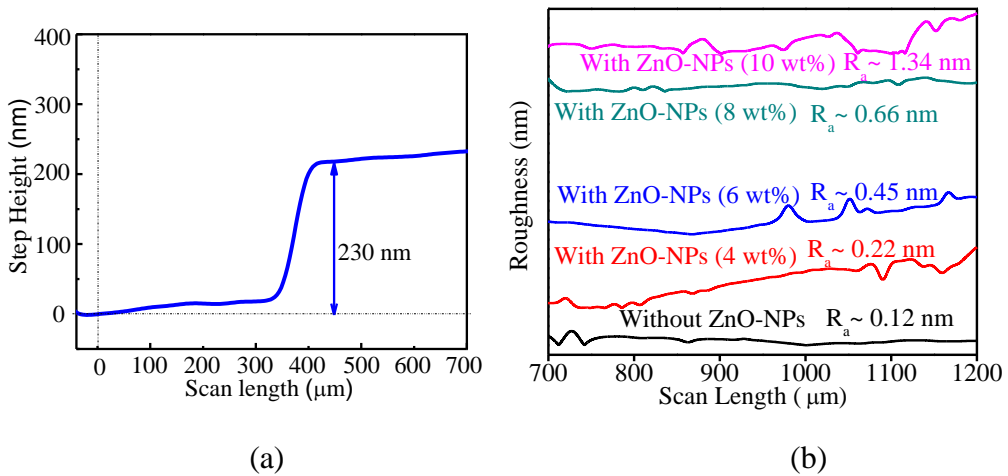


Figure 6: (a) Step height profile of MEH-PPV:PCBM photoactive layer. The thickness is about 230 nm and (b) Roughness profiles for the MEH-PPV:PCBM films with and without ZnO-NPs.

Table 1: Measured device parameters of pure MEH-PPV:PCBM and MEH-PPV:PCBM/ZnO-NPs solar cells.

MEH-PPV:PCBM Device	V _{oc} (V)	J _{sc} (mA/cm ²)	FF	PCE (%)
Without ZnO-NPs	0.63	67×10 ⁻²	26.40	11.20×10 ⁻²
With ZnO-NPs (4 wt%)	0.58	0.04×10 ⁻²	22.81	0.01×10 ⁻²
With ZnO-NPs (6 wt%)	0.49	0.10×10 ⁻²	22.91	0.01×10 ⁻²
With ZnO-NPs (8 wt%)	0.63	7.19×10 ⁻²	16.99	0.77×10 ⁻²
With ZnO-NPs (10 wt%)	0.71	0.82×10 ⁻²	11.68	0.07×10 ⁻²

Table 2: The series resistance (R_s) of the device and average roughness (R_a) of MEH-PPV:PCBM photoactive layer with and without ZnO-NPs.

MEH-PPV:PCBM Device	Average roughness R _a (nm)	Series resistance R _s (Ωcm ²)
Without ZnO-NPs	0.12	0.87
With ZnO-NPs (4 wt%)	0.22	15.62
With ZnO-NPs (6 wt%)	0.45	15.54
With ZnO-NPs (8 wt%)	0.66	18.18
With ZnO-NPs (10 wt%)	1.34	113.25

Conclusion

The additive "ZnO-NPs concentration of 8 wt%" provides the highest absorption intensity. Achieving the high optical absorption is requisite for photoactive layers in solar cells. This work involves the fabrication of organic solar cells using MEH-PPV/PCBM polymer blend film as photoactive layer. The effects of additive (ZnO-NPs) concentration on device efficiency were investigated. The device using "dichlorobenzene" produced the efficiency as high as 0.112% (open circuit voltage 0.63 V, short circuit current density 0.67 mAcm⁻² and fill factor 26.40). The obtained device efficiency was correlated to the properties of the photoactive films. Despite having higher

absorption in active layer with ZnO-NPs, the efficiency of this modified device underperformed the reference device (without ZnO-NPs) which is attributed to the restricted charge carrier transport and morphological perturbation.

Acknowledgement

The author would like to thank Dr Thura Oo, Rector, Monywa University, for his invaluable guidance. The author gratefully thanks to Dr Thet Naing Oo and Dr Sein Sein Aung, Pro-Rectors, Monywa University, for their advice. The author also gratefully thanks Professor Dr Shwe Zin Aung, Head of Department, Department of Physics, Monywa University, for her permission and valuable suggestions.

References

- B. Chung *et al.*, Appl. Phys. Lett. **55** (1989) 1741.
- C. J. Neef and J. P. Ferraris, Macromolecules **33** (2000) 2311.
- C. Tang *et al.*, Appl. Phys. Lett. **91** (2007) 143.
- C. Ton-That *et al.*, Solid State Mat. Sci. **6** (2002) 87.
- G. Zhang *et al.*, Appl. Phys. Lett. **94** (2009) 143.
- J. Kim *et al.*, J. Science **45** (2007) 222.
- K. Wu, "Master Thesis", McMaster University (2010).
- N. Shaheen *et al.*, Appl. Phys. Lett. **78** (2001) 98.
- S. H. Yang, Adv. Mater. Sci. **15** (2007) 27.
- X. Wang *et al.*, Front. Chem. Lett. **5** (2010) 45.